Tripodal penta(*p*-phenylene) for the biofunctionalization of alkynyl-modified silicon surfaces

María Sánchez-Molina,[a] Amelia Díaz,[a] María Valpuesta,[a]
Rafael Contreras-Cáceres,[a] J. Manuel López-Romero, [a,*] M. Rosa López-Ramírez [b]
a) Dep. Química Orgánica, b) Dep. Química Física
Facultad de Ciencias, Universidad de Málaga, 29071 Málaga, Spain
*jmromero@uma.es

Abstract

Here we report the optimization on the covalent grafting methodology of a tripod-shaped penta(*p*-phenylene), **1**, on alkynyl-terminated silicon surfaces, and the incorporation of an active theophylline derivative, **2**, for the specific immobilization of proteins. The tripodal molecule presents azide-terminal groups to be attached onto a silicon surface containing an alkynyl monolayer. Initially, compound **1** has been covalently incorporated on alkynyl-terminated Si wafers, by the copper catalyzed alkyne-azide 1,3-dipolar cycloaddition (CuAAC, a click reaction). The tripod density on the silicon surface is tuned by performing the CuAAC reaction at different concentrations of **1**, as well as under different experimental conditions (T, base, copper source, shaking). Then, tripod **1**-modified surface has also been biofunctionalized with **2**. The effective preparation of this silicon-modified surface allowed us to study the streptavidin immobilization on the surface. Characterization of the different surfaces has been carried out by X-Ray Photoelectron Spectroscopy (XPS), Atomic Force Microscopy (AFM) and Bright-Field Optical Transmission Microscopy (Confocal) techniques. We also include density functional theory (DFT) analysis of the organic structures to confirm the height-profile and the tripod-surface relative configuration extracted from AFM images.

Keywords: tripodal phenylene; silicon surface; click reaction; nanostructuration; theophylline; bifunctionalization

1. Introduction.

During the last years the development of molecularly ordered surfaces to be applied in research fields as protein adsorption, clinical diagnostics or cellular adhesion, has been extensively reported.[1] A great number of approaches are currently investigated to generate ordered arrangements at the molecular level with the aim to replicate biochemical reactions on solid supports. Among a vast number of procedures for surface functionalization as electron-beam lithography,[2] assembly of supramolecular aggregates,[3] nanoparticles as templates,[4] or molecular modification of AFM tip for ligand-receptor AFM force spectroscopy,[5] the generation of self-assembled monolayers (SAMs) has been widely employed for the fabrication of functionalized thin films on a wide range of surfaces as Au, Al_2O_3, SiO_2, TiO_2 or Si, being the latter less studied.[6] By SAMs approach, the incorporation of active functional moieties can be easily performed at the molecular level in a controllable and reproducible way. Indeed, by this method it is possible to tune the space between grafted functional groups on surfaces, which offers the possibility to fabricate interfacial architectures in bio-devices with molecular precision for the interaction with cells or certain biomolecules in a highly specific manner. To date, several macromolecular architectures focused on SAMs have been deeply investigated to provide functional molecular platforms to be used as templates for different applications ranging from tissue engineering,[7] medicine,[8] cell biology,[9] immunology,[10] and marine biofouling.[11] For instance, the adsorption of substituted porphyrin molecules for the construction of bioorganic model systems,[12] or triazatriangulenium ions as platforms on metal surfaces with precise tuning of the intermolecular distances between the adsorbates,[13] have been performed for the controlled orientation of the functional groups relative to the surface. Dendrons are a class of tree-like architectures, which are able to self-organize into 2D arrangements.[14]

These branched molecules have also been anchored on different surfaces providing multiple functional sites for further functionalization. Some of these dendron-modified substrates are able to exhibit controlled surface wetting, revealing a surface polarity memory effect. They have been also used for the fabrication of a surface for efficient catalysys of styrene hydrogenation.[15]

Concerning 2D arrangements, an useful alternative strategy is the use of tripodal molecules as binding units, which can cover a specific area and control lateral spacing after being attached on different surfaces. Depending on the tripod size, they will be able to significantly guarantee the spatial arrangement between the self-standing functional arms that protrudes from the surface. Tripod-shaped molecules, susceptible to form SAMs, commonly have several phenyl[16] or phenylacetylene[17] units on each tripod-leg bearing the anchor groups, while the fourth leg is the tail group (also named functional arm) that might be further functionalized.

In this regard, CuAAC reactions[18] in solution have become a successful tool for the functionalization of a wide range of metal surfaces that have been previously modified by alkynyl or azido groups.[19] In a preliminary work, we covalently attached tripod-shaped tri(*p*-phenylene)s on alkynyl-terminated silicon wafers in a highly ordered distribution by using CuAAC conditions for potential application in the specific adsorption of proteins.[20] This type of protein immobilization at surfaces is of great importance in a number of applications, including surface-based bioassays,[21] biosensors,[22] clinical diagnosis and biomedical devices such as implants.[23] In this case, the modified-surfaces must be fabricated to present functional moieties that can specifically interact with proteins while avoiding interaction with all other proteins. For example, theopyllines are methylxanthine derivatives with pharmacological

applications, which have been used as templates for the specific incorporation of proteins due its extensively affinity for streptavidin.[24]

Here we present the optimization of the covalent grafting of tripod-shaped molecules (compound **1**) on alkynyl-modified silicon substrates by CuAAC reaction. In order to define the optimal conditions for silicon surface nanostructuration, we have analyzed in depth the influence of experimental variables as the tripod concentration, reagents and solvents, as well as temperature and shaking during the preparation. Then, the tripod **1**-modified nanostructured templates were tested for the covalent incorporation of theophylline active molecules (compound **2**), also by CuAAC reaction. Finally, the behavior of these surfaces for streptavidin immobilization has been achieved. According to XPS and AFM analysis, the presence of the penta(*p*-phenylene) **1** onto the alkynyl-terminated silicon surfaces is demonstrated. We included (DFT) analysis that confirms the height profile and the tripod-surface relative configuration obtained from AFM images. Confocal microscopy and XPS analysis were used to monitorize the specific streptavidin-surface interactions.

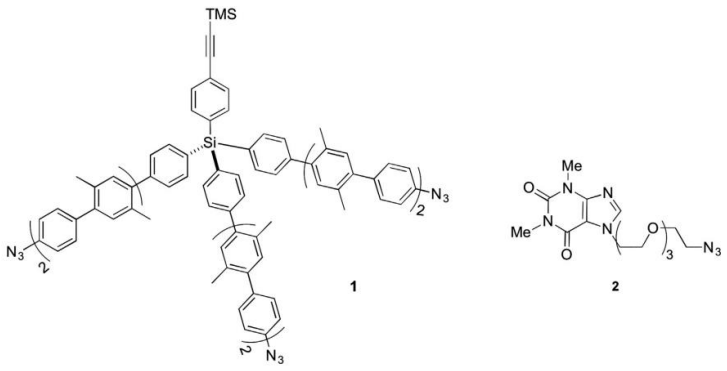

Figure 1. Penta(*p*-phenylene) tripod **1** and theophylline derivative **2**.

2. Experimental.

2.1 Materials.

Starting materials and reagents were purchased from Aldrich and used without further purification. Compounds **3** and **4** (4,7,10,13,16-pentaoxaheptacos-26-en-1-yne) were prepared following the previous reported procedure.[28] Tripod **1** was synthesized by Suzuki-coupling of corresponding boron esters, according to the published procedures.[20,25] Tetrahydrofuran (THF) was dried and distilled from sodium benzophenone under an argon atmosphere, and dichloromethane was dried and distilled from CaH_2 under an argon atmosphere. Millipore water was used when needed.

2.2 Characterization methods.

XPS was performed on a PHI 5700 X-ray photoelectron spectrometer equipped with a monochromatic AlKa X-ray source (1486.7 eV) at a takeoff angle (TOA) of 458 from the film surface. The spectrometer was operated at both high and low resolution with window pass energies of 23.5 and 187.85 eV, respectively. Electron binding energies were calibrated with respect to the C 1s line at 286.4 eV (C/C) or the Si 2p line at 99.0 eV. Signal deconvolution was performed first by Shirley background subtraction, followed by nonlinear fitting to mixed Gaussian-Lorentzian function with 80 % Gaussian and 20 % Lorentzian character.

AFM imaging of the surfaces was performed on a Multi Mode Nanoscope V AFM (Digital Instrument Inc., Santa Barbara, California). Images were acquired in tapping mode by using a silicon nitride cantilever (MikroMasch, San Jose, California) with a resonant frequency of 132.9 kHz and a nominal force constant of 1.75 Nm^{-1}.

Fluorescence images were taken on a Leica TCS SP5 Confocal (Leica). We characterized the localized emission fluorescence from 1 cm x 1 cm surfaces between 550-650 nm, excited with a laser at 458 nm using 20x objective.

The ellipsometric box model GES-5E Sopra-Semilab was used for thickness measurements, at λ = 632.8 nm, and incidence angles of 60, 65 and 70º. Data were analyzed by using the WinElli2 software, applying a multilayer optical model, and tabulated n and k constants for Si(111). Cauchy dispersion laws have been used for modeling surfaces $n\lambda=A+B\lambda^2$. Thickness values are the average of measurement made from the three mentioned angles in one point of the modified wafers. All measurements were obtained with an R^2 value in the interval 0.9989 and 0.9982.

2.3 Preparation of H-Si(111) substrates and fabrication of alkynyl-terminated Si wafers (surface A).

Single-side polished, p-type (boron-doped, 1-10 Ω/cm resistivity) Si(111) wafers (Silicon Quest International, Inc.) were cut into pieces of 1 cm x 1 cm and cleaned with Piranha solution (concentrated H_2SO_4/30 % H_2O_2 3:1 v/v) for 30 min at 80 ºC to remove impurities. *Caution: Piranha solutions react violently with organic materials and should be handled with extreme care*. In order to reduce the SiO_2 substrate to H-Si, the freshly cleaned sample was immersed in an argon-saturated, 2.5 % HF solution for 10 min, followed by rapid rinse with argon-saturated water and dried with a stream of argon.

The freshly prepared 1 cm x 1 cm H-Si(111) substrate was placed in a simple vacuum chamber setup combining a Schlenk tube with a quartz cell for photo-induced surface hydrosilylation. The H-Si(111) sample was put in contact with a droplet of **3** on a quartz disk, forming an uniform layer of the molecule sandwiched by the quartz disk and the

silicon slide. Hydrosilylation process was carried out at 254 nm UV light illumination during 2 h at atmospheric under high vacuum condition (0.05 mbar). The substrates were finally washed sequentially with ethanol and CH_2Cl_2, and finally dried with a stream of argon to obtain surface A (Scheme 1).

2.4 CuAAC reaction of 1 onto alkynyl modified H-Si(111) (surfaces B).

The grafting of **1** was performed by CuAAC click reaction onto freshly prepared Si-alkynyl surfaces (surface A) obtaining surfaces B. We have performed the reaction by using two different copper salts and two different bases (procedures a and b). *Procedure a)* reaction was carried out in a similar manner as we previously reported.[28] Briefly, a 0.5 mm x 0.5 mm piece of surface A was immersed into a degassed THF/MeOH (1:1 v/v) solution containing $Cu(MeCN)_4PF_6$ (3.75 mM), **1** (5 mM) and the copper ligand **4** (37.5 mM) during 24 h at room temperature. *Procedure b)* a 0.5 mm x 0.5 mm piece of surface A was immersed into a degassed THF (2 mL) solution containing CuI (catalytic amount), **5** as base and **1** (see Table 1). Table 1 also summarize the temperature and if shake is carried out. After incubation during 24 h, the sample was taken out and immersed into aqueous EDTA solution (5 mL, 25 mM), sonicated for 10 s, and thoroughly washed with water, then ethanol and finally dried with a stream of argon, obtaining surfaces B.

2.5 CuAAC reaction with theophylline 2 onto deprotected 1-Si-surfaces (surfaces C).

A 0.5 mm x 0.5 mm sample of surface B5 was immersed into a degassed methanol (5 mL) solution containing K_2CO_3 (1 mM), then shaked for 1 h at room temperature. After this period, the sample was taken out and thoroughly washed with water, then ethanol

and finally dried with a stream of argon. After drying, sample was immersed into methanol (5 mL) solution containing CuI (catalytic amount), **5** (500 mM) and **2** (5 mM). After 24 h reaction at room temperature, the sample was taken out and immersed into aqueous EDTA solution (5 mL, 25 mM), sonicated for 10 s, and thoroughly washed with water, then ethanol and finally dried with a stream of argon, obtaining surfaces C.

2.6 Protein immobilization.

Pieces of pristine and processed SAMs (surface C) were immersed in a solution of streptavidin (0.5 mL, 1 ng/μL) in PBS-buffer (pH= 7.4) and slowly stirred (protected from light) at 25 ºC for 1 h. After immersion, the samples were washed with water and dried in a stream of argon and kept in a desiccator, and then they were kept in cold (surfaces D).

3. Results and discussion.

Grafting tripod-shaped molecules on modified silicon surfaces has proven to be very dependent on experimental conditions and only around 30 % yield is usually obtained concerning the surface coverage.[26] This circumstance can be explained by a partial reaction of alkyne and azide groups resulting in unbound legs, which has been observed mainly when alkynyl groups are attached to the surface.[27] Despite this, and since we have previously obtained good results for the attachment of a small tripod (three phenylene units) on alkynyl modified silicon surfaces, in this work we initially prepared the penta(*p*-phenylene) modified surfaces by following the same procedure.[20] The clickable silicon surfaces were prepared by photo-activated hydrosilylation reaction of the alkene derivative **3** onto H-Si(111) substrates (Surface A in Scheme 1).[28] Then,

tripod **1**-modified silicon surfaces were prepared by CuAAC reaction onto the previously prepared surfaces in presence of **1**, a copper source and a base (Surface B in Scheme 1).

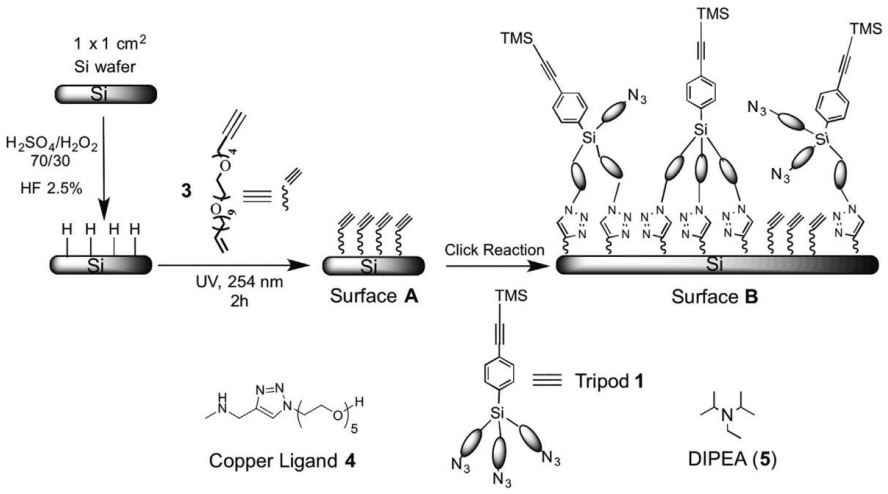

Scheme 1. Representation of tripod **1** grafting onto alkynyl-modified H-Si(111) substrates.

For the preparation of surface B, the optimum base/copper source/solvent combination in CuAAC reaction was analyzed. Initially, $Cu(MeCN)_4PF_6$ was used as copper source together with **4** as a base, in a methanol/THF mixture at room temperature, thus resulting in surface B(**4**) (entry 1, Table 1).[20] At the same time, due to the poor solubility of the tripod **1** in methanol, we analyzed the effect of changing the solvent using only THF along together with new copper salt (CuI) and base (*N*,*N*-diisopropyletilamine, DIPEA, **5**), since previous Cu-complex is not soluble in THF, obtaining surface B(**5**) (entry 2, Table 1). In both cases the concentration of tripod **1** used during the CuAAC reaction was 5 mM.

Table 1. Concentration of tripod **1**, copper source, base, solvent and conditions used in the different CuAAC reactions performed onto alkynyl-terminated surfaces.

Entry	Tripod **1** [mM]	Copper Source	Base [mM]	Reaction Solvent	Shaking	Temp.	Surface
1	5	$Cu(MeCN)_4PF_6$	**4**, 37.5	THF/MeOH	No	RT	B(**4**)
2	5	CuI	**5**, 500	THF	No	RT	B(**5**)
3	0.05	CuI	**5**, 5	THF	Yes	35ºC	B1
4	0.05	CuI	**5**, 5	THF	Yes	RT	B2
5	0.05	CuI	**5**, 5	THF	No	RT	B3
6	0.5	CuI	**5**, 50	THF	No	RT	B4
7	0.25	CuI	**5**, 25	THF	No	RT	B5

As commented above, the presence of tripod **1** on the alkynyl-terminated surfaces was initially studied by XPS measurements (Figure 2). The XPS spectrum corresponding to the untreated H-Si(111) substrate only shows a narrow Si2p peak at 99.3 eV, with no presence of SiOx species in the 102-104 eV region (Figure 2a). Figure 2b and 2c shows XPS survey scan for surface B(**4**) prepared with $Cu(MeCN)_4PF_6$/**4**/MeOH/THF and surface B(**5**) under CuI/**5**/THF conditions (entries 1 and 2, respectively, Table 1). By XPS analysis, surface B(**4**) is composed by C 1s (60.91 %), N 1s (1.74 %), O1s (18.98 %) and Si 2p (17.45 %), and surface B(**5**) by C 1s (80.5 %), N1s (2.84 %), O1s (10.6 %) and Si 2p (3.57 %). As it is observed, in surface B(**5**) the amounts of C 1s and N 1s are higher when compared with that for surface B(**4**). Moreover, the percentage of Si 2p after CuAAC reaction is remarkably lower for surface B(**5**) in comparison with surface B(**4**). It means a more homogeneous tripod grafting and a better covering density in surface B(**5**). We have calculated the yields for both CuAAC reactions.[28] This parameter is derived from $(C/N)_{XPS} = (22 + 113 \cdot Y) / 9 \cdot Y$, where Y is the reaction yield (%), C/N is the intensity ratio measured by XPS, 22 is the number of C atoms before the CuAAC reaction, 9 is the number of N atoms in the azide, and 113 is the number of C atoms in the tripod deposited after CuAAC reaction. On the base of the C/N ratio, the CuAAC reaction yield was estimated to be 25.9 % for surface B(**4**). This value is lower than the

one obtained in our previous work concerning tripodal-shaped oligo(*p*-phenylenes) with three phenylene units (31.2 %), using the same cooper salt.[20] On contrary, by performing the CuAAC reaction with CuI and **5** the reaction yield remarkably increases up to 52.0 % (surface B(**5**)). This increment is probably produced due to the higher solubility of the tripod **1** in THF, instead of using a MeOH/THF mixture.

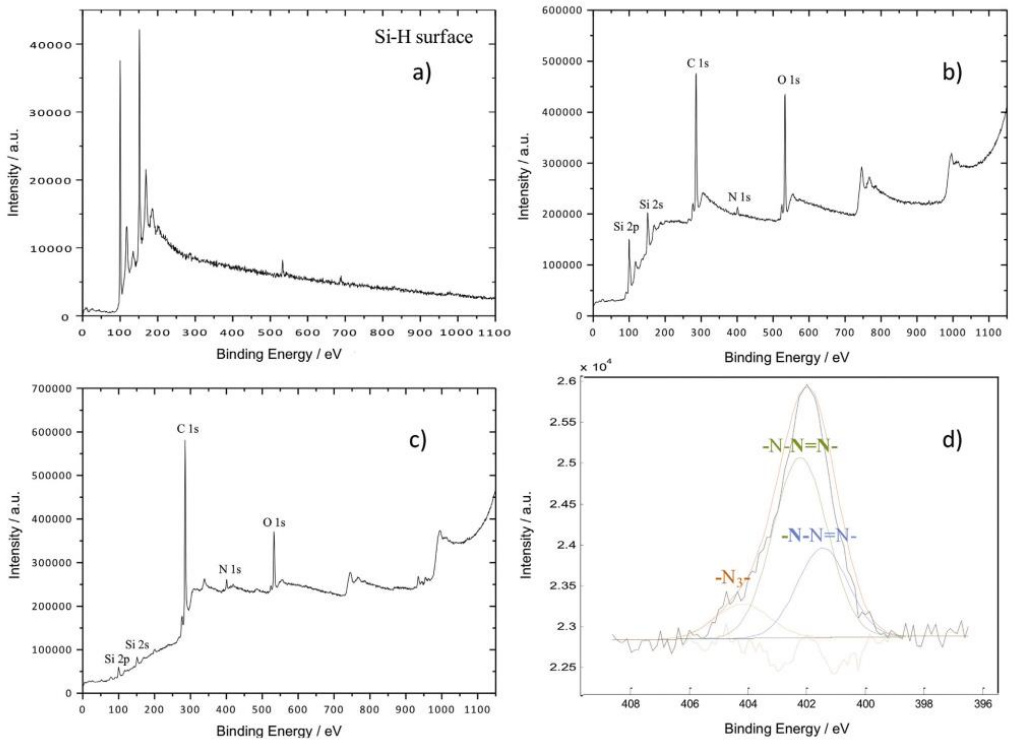

Figure 2. XPS survey scan for a) a pristine H-Si(111) surface; b) surface B(**4**) prepared under conditions shown in entry 1, Table 1 ($Cu(MeCN)_4PF_6$/**4**); c) surface B(**5**) prepared under conditions shown in entry 2, Table 1 (CuI/**5**). d) XPS narrow scan of the N 1s region for surface B(**5**).

It is important to note that the XPS analysis also demonstrates the presence of the triazole group after CuAAC reaction. Figure 2d represents the deconvolution of the N 1s narrow scan for tripod **1** grafted on surface B(**5**) (entry 2, Table 1, surface B(**5**)), where the three different bands are obtained. First two, at 400.5 eV (-**N**-N=N-) and 401.7 eV (-N-**N=N**-), are assigned to the triazole group, being 1:2 the calculated ratio for these areas, respectively, as extracted from the N 1s narrow scan, which is consistent with the stoichiometric ratio. Moreover, the band at 403.0 eV corresponds to free azide

groups not grafted to the terminal triple bond. The calculated ratio for this area with respect to that of the triazol group is 1:7, meaning that only 12 % of free azide groups are presented on the modified surface.

We can conclude that the use of CuI/**5**/THF combination provides better results for the Si surface modification with **1**. Then, morphology of the prepared surface B(**5**) was analyzed by tapping mode in AFM technique (Figure 3a,b). Even when good yields for the CuAAC reaction were obtained, poor results are found regarding parameters such as monolayer thickness and nanostructuration extent. In fact, when this surface was analyzed by AFM (Figure 3), it was found a thickness corresponding to multilayer deposition: an almost complete silicon surface coverage with height reaching a maximum peak height of 46 nm, and an average of 10 nm. Figure 3c and 3d also show AFM images of a just-etched and clean Si(111) wafer and an alkynyl modified silicon surface (Surface A, Figure 3d). Roughness values for these surfaces are 0.57 nm over an area of 25 μm^2 (Figure 3c) and 0.25 nm along 0.25 μm^2 (Figure 3d).

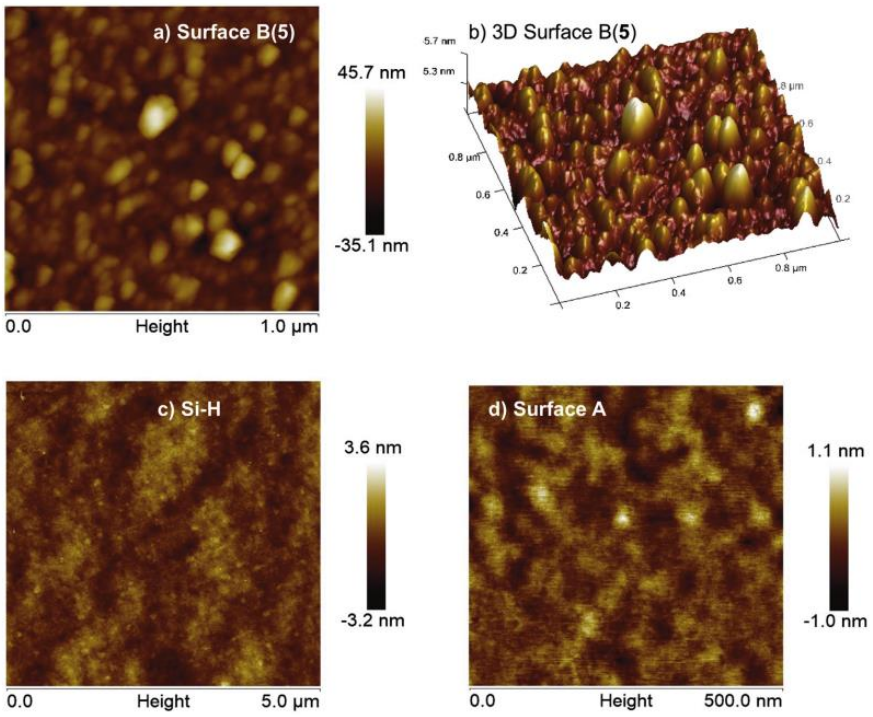

Figure 3. Tapping mode 2D and 3D AFM images of surfaces Si(111), A and B(**5**).

This result prompted us to optimize not only the concentration of **1** used in the CuAAC reaction, but also the reaction temperature and if the substrate is subjected to shake while the reaction is carried out. Reactions were performed by using CuI, compound **5** and a 0.05 mM solution tripod **1** as a mixture of reagents, and THF as solvent, at different experimental conditions (entries 3, 4 and 5 in Table 1, surfaces B1, B2 and B3). In Figure 4, we include representative tapping mode 2D and 3D AFM images, corresponding to surfaces B1, B2 and B3.

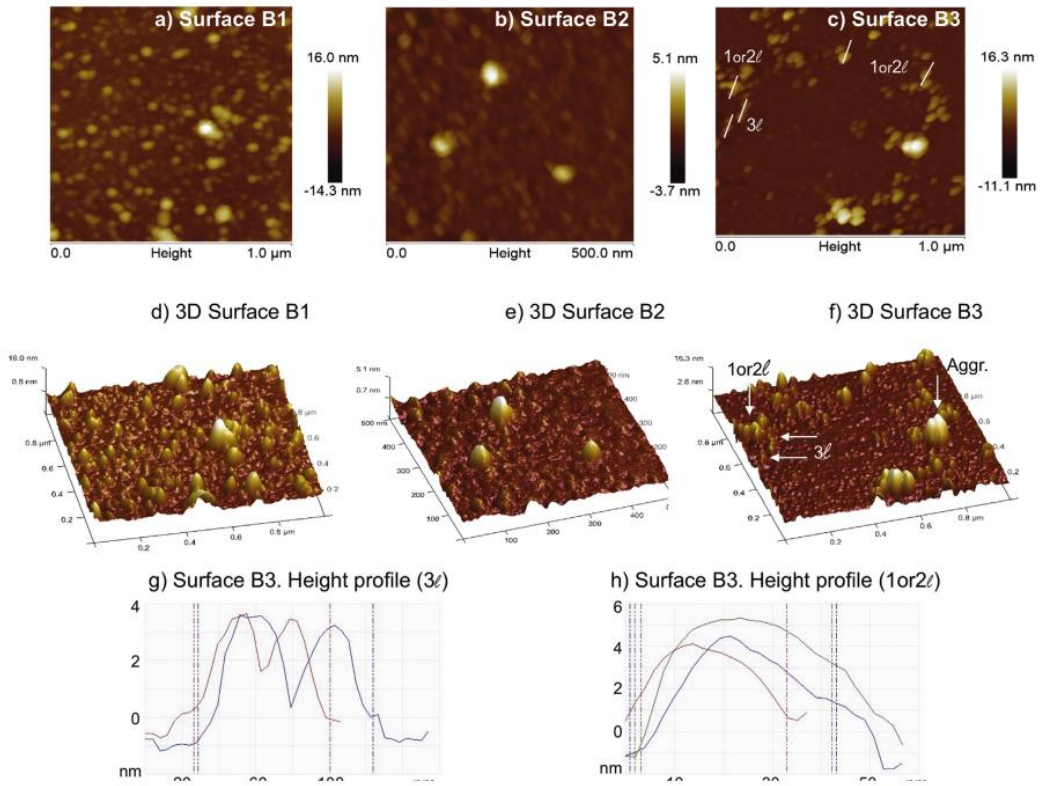

Figure 4. Tapping mode 2D and 3D AFM images (1 x 1 µm) of the alkynyl-terminated silicon wafer after incorporation of a solution 0.05 mM tripod **1** at several concentrations by CuAAC reaction, and height profile of several tripods extracted from AFM images: tripods attached by the three legs (3l) and by one or two legs (1or2l).

As can be observed, in all cases the alkynyl-terminated silicon surfaces presented tripod-shaped structures grafted on it (Figure 4). 3D AFM images display in a better detail both the morphology of the molecule attached on the silicon surface as well as the

height of the incorporated tripod. Images 4a,d correspond to the surface B1 prepared by heating at 35 ºC and shaking; images 4b,e correspond to the surface B2, obtained under shaking and at room temperature; and images 4c,f correspond to surface B3 with tripods grafted at room temperature and no-shaking conditions (entries 3, 4 and 5, respectively, in Table 1), all of them prepared from a 0.05 mM solution of **1**. As can be seen in Figure 4, surface B1 presented an improved tripods distribution with a lower aggregation that those prepared with higher concentrations of **1** (5 mM, surface B(**5**)). Moreover, surfaces with low tripods aggregation are a common result obtained with 0.05 mM concentration (surfaces B2 and B3). Surface B2, which represents an alkynyl-terminated silicon surface, after CuAAC reaction carried out under shaking and at room temperature, presented a lower amount of tripods but in a well-defined distance between them, with no aggregation. Separation of tripods for this surface was estimated in an average of around 360 nm. Surface B3, which represents 0.05 mM concentration of **1** without shaking and at room temperature, it shows low amount of tripods and few irregular aggregates after grafting. It is important to mention that, as was previously reported,[20] these azide-terminated penta(*p*-phenylene) tripods can be attached on a alkynyl-terminated surface by one, two or the three azide groups. In this work, we are interested in finding the conditions that provide tripods linked by the three legs (three azide groups), since this configuration allows incorporating the theophylline derivative perpendicular to the silicon surface (see Scheme 1). We have established the height of the tripods deposited on the silicon surfaces by analyzing the high profile from AFM images (Figure 4g,h), which have been later compared with the height obtained by DFT calculations (see Figure 6). We estimate in 3.4 nm height for tripod attached to the surface with the three legs, and 4.0 nm and 5.5 nm when is attached with only two and one, respectively.

In surface B3 (Figure 4c,f) we have indicated the tripods attached as bilayer or aggregates, and tripods attached by one, two or three legs (arrows), and the resulting high profiles confirmed a higher number of tripods attached by the three legs, compared with the other conformations. On the other hand, in surface B1 we can observe several tripods deposited as bilayer or aggregates, and the number of tripods deposited with one or two legs is higher compared with that for tripods attached by the three legs.

Therefore, at same concentration values, shaking difficult the adsorption of adsorbates to the surface by the three legs, while heating speed up the process but also leads to obtain aggregates. No heating and no shaking seem to be the better experimental conditions for the preparation of ordered tripod surfaces with our desired configuration (surface B3).

However, by carrying out the surface preparation with solutions of low tripod-**1** concentrations (0.05 mM), poor surface coverages are obtained. We studied the CuAAC reaction with concentrations of **1** in the range of more concentrated solutions, 0.5-0.05 mM (Figure 5). Surface B4 (Figure 5a, b and c) represents substrates with 0.5 mM of **1**, without shaking and at room temperature (entry 6, Table 1). In this case the amount of tripods is higher when compared to the previous cases, the grafting density is higher, and now tripods are in contact between them. However, if we observe the image at the lower magnification (Figure 5a) tripods form aggregates which are randomly distributed on the silicon surface. Apart from that, the high profile extracted from AFM images shows a low amount of tripods attached by the three legs, compared to the other possible configurations.

Surface B5 (Figure 5d, e and f) corresponds to a sample with a tripod concentration of 0.25 mM prepared without shaken and at room temperature (entry 7, Table 1). The image at low magnification shows a well-distributed tripod configuration and a higher

amount of tripods grafted on the silicon surface was obtained if compared with the previous one at 0.05 mM. Indeed the image (Figure 5e) shows a large number of tripods attached by the three legs in comparison with the other possible configurations. We can conclude that, even when the grafting density is higher (surface B4), the homogeneity of the surface is better in surface B5, with almost absence of random aggregates, and with a higher amount of tripods attached by the three legs. Surface B5 was also analyzed by ellipsometry. A thickness of 1.87 ± 0.0348 nm of native Si-alkyne was measured by means of this technique, while measurements determined a thickness of 2.94 ± 0.1173 nm for the tripod **1** monolayer in surface B5.

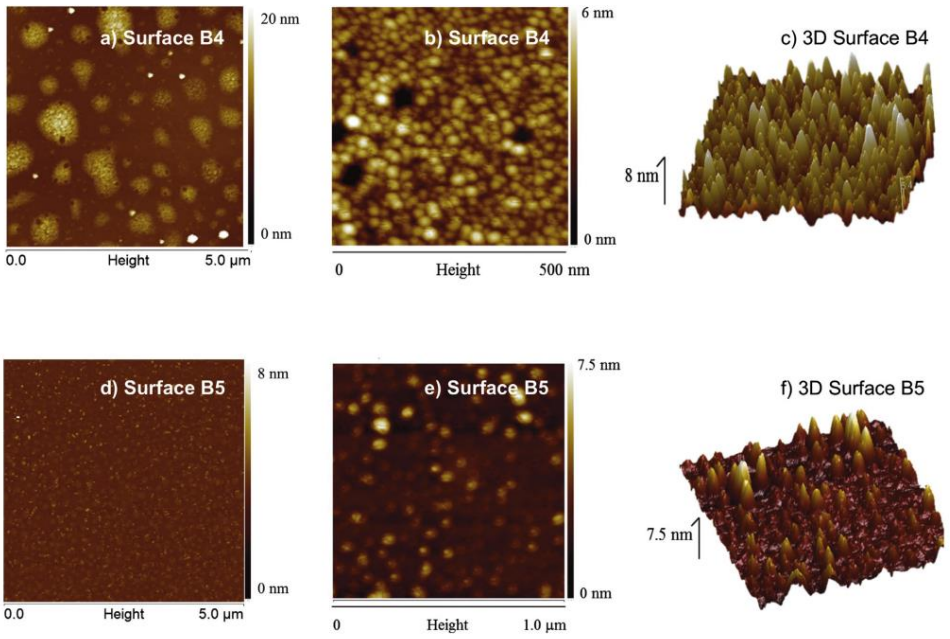

Figure 5. Tapping mode 2D and 3D AFM images of the alkynyl-terminated silicon wafer after incorporation of tripod **1** at 0.5 (surface B4, roughness: 2.95 nm) and 0.25 mM (surface B5, roughness: 1.25 nm) concentrations by CuAAC reaction.

The structure and possible orientations of the tripod **1** on the surface have been analyzed by DFT calculations. Figure 6 includes DFT optimized geometries for **1** in gas phase and grafted on the silicon surface at the three possible configurations. We have denoted (*a*) the distance between azide group and the Si core, (*b*) the distance between two

azides groups, (*c*) the distance between an azide and the TMS group, and (*d*) the distance from the alkynyl group and the base of the tripod, being the calculated distances 25.0, 39.5, 30.4 and 31.1Å, respectively (gas phase).

Surface B in Scheme 1, represents the three possible different final conformations of the grafted tripod on the alkynyl-terminated silicon surface after CuAAC reaction. We have also used DFT analysis to calculate the high of each tripod attached to the surface taking into account the three relative grafting possibilities (Figure 6).

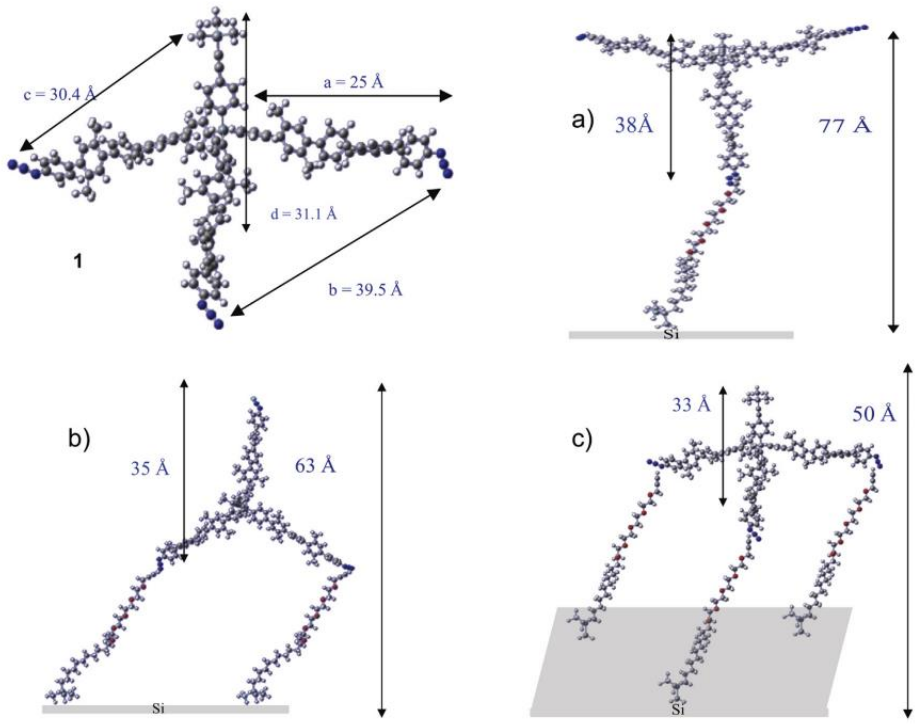

Figure 6. a) Draw of tripod **1** denoting main DFT calculated dimensions, and optimized geometries representation of possible orientations of tripod **1** on alkynyl-terminated Si(111) surface: b) only one bound, c) two and d) three.

Figure 6b-d represents the optimized geometries for tripod **1** grafted on the surface by one, two or three azide groups, respectively. As we deduced from AFM images the final tripod height is different for each conformation. The **1**-calculated heights from the silicon surface (comprises compound **3** and tripod **1**, molecules) are 77, 63 and 50 Å, respectively. Is important to mention that for DFT calculations, the total height is not

the same from that extracted in the 3D AFM images. DFT calculations include one, two or three molecules of compound **3**, so the angle in which it is attached on the silicon wafer is different, resulting in different thickness. On contrary, for our experimental conditions, the thickness of the silicon surface after compound **3** incorporation (Surface A in Scheme 1) measured by ellipsometry was 24 Å. As it can be observed, the calculated height of **1** (distance from the base of the tripod to the TMS group) is higher when is attached to the surface (33.0 Å) than when it is calculated in solution (31.1 Å, 3.1 nm). This fact can be attributed to a more rigid configuration when the position of the three legs is fixed to the surface. In any case, the calculated height is in concordance with the measured tripod **1** height of 3.4 nm in surface B3. It also means a possible uncompleted attachment of the three legs of tripod **1** to the Si in surface B2 since the height observed in tripod is closed to 6 nm, and a high percentage of this situation is found on surface B1. This fact can be attributed to shaking conditions. Moreover, based on height measurements, in surface B3 only 10 % of tripod molecules are attached to the surface only by one or two legs, concluding that most of the tripods (90 %) are attached through the three azide points to the silicon surface B3. Similar result is obtained for surface B5, so we can conclude that grafting at room temperature without shaking and using a 0.25 mM concentration of **1** lead us to achieve good homogeneity on the surface, with almost the absence of random aggregates, and with most of the tripods attached by the three legs to the surface. Consequently, and as we have mentioned above, surface B5 is the appropriated for theophylline incorporation.

3.1 Theophylline attachment and protein adhesion study.

Theophylline is a molecule with many known activities, including formation of complexes with DNA, serving as a strong antioxidant that prevents DNA damage,[29] or

the high affinity with a family of adenosine receptors known as A_1, A_{2A}, A_{2B}, and A_3.[30] Their derivatives are also well known to influence neuronal activities by binding with the above adenosine receptors.[31] A theophylline-oligo(ethyleneglycol)-alkene derivative presenting activity against adenosine receptors[32] has been incorporated onto poly(vinylidene fluoride) and regenerated cellulose membranes. It can be also used to monitorize streptavidin interactions when adsorbed on polymeric support.[33,24] However, by using these polymeric systems, random interaction between theophylline derivative and surfaces were observed.

Our approach prepares silicon substrates with azido-terminated theophyllines based on CuAAC chemistry. For this purpose, the terminal alkynyl group on the functional arm of tripod **1** was here deprotected by removing TMS groups under basic conditions, such as K_2CO_3 in methanol. Removing trialkyl silyl groups on monolayer has previously been carried out with F^- in various solvents, in a sluggish method that requires high concentration of F^-, long reaction time and high temperature.[19c] However, by using K_2CO_3 in methanol, TMS groups can be removed under very mild conditions. In our work, the subsequent attachment of the azido-terminated theophylline **2** was carried out over the deprotected surface B5, employing the optimized CuAAC conditions for tripod **1**, thus resulting in surface C (Scheme 2).

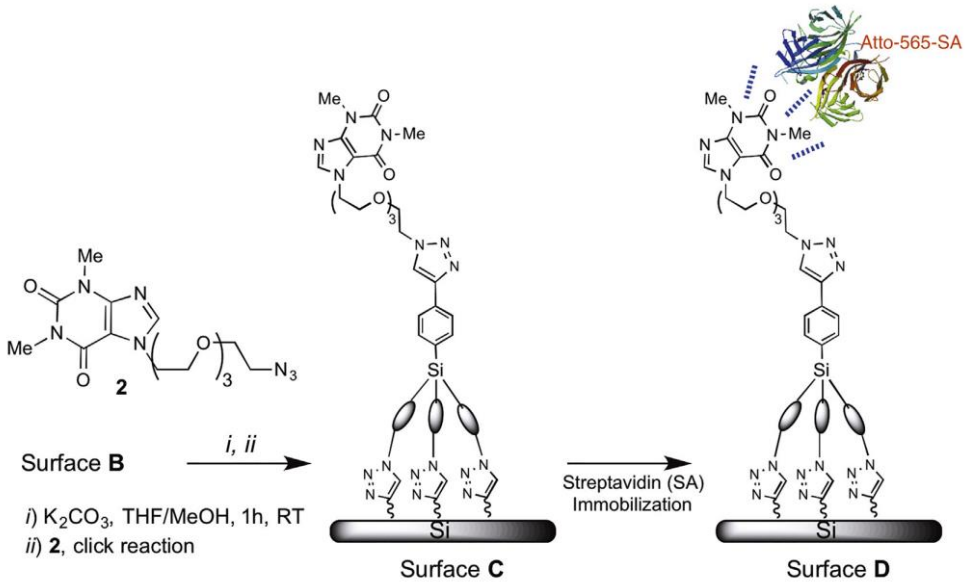

Scheme 2. Covalent attachment of the theophylline **2** on an optimized silicon surface with tripod **1** and subsequent streptavidin adhesion.

Upon grafting the theophylline **2** onto the **1** terminated surfaces, bioactivation of these surfaces is demonstrated performing protein adhesion test. The samples were incubated in solutions of conjugated ATTO-565 streptavidin (SA) in phosphate aqueous buffer (PBS). XPS investigation confirmed the presence of the theophylline derivative and the incorporation of streptavidine on the on the tripod-modified surface. Figure 7 shows the N 1s scan for tripod-modified silicon surface (surface B5, black line), after theophylline incorporation (surface C, red line) and after streptavidin treatment (surface D, blue line), respectively. As can be observed, the N 1s signal intensity increased from surface B5 to surface C due to the presence of both the triazol groups provided after the CuAAC reaction and the nitrogen atoms included in the theophylline derivative **2**. After streptavidin treatment, the remarkably increase of the N 1s intensity is attributed to adsorbed protein.

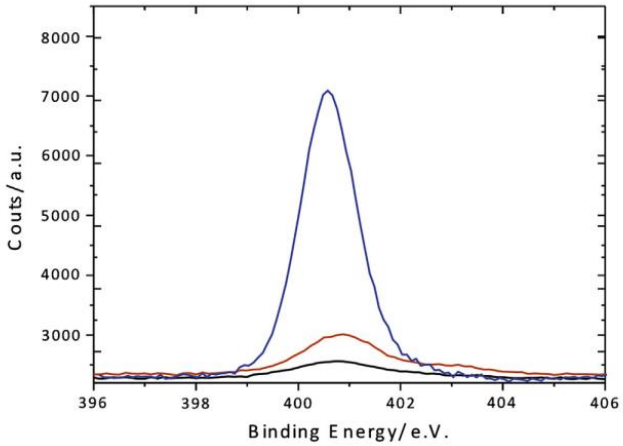

Figure 7. N 1s scans for surface B5 (black line), surface C (red line) and surface D (blue line).

Selective binding of the protein to the surface has been analyzed by bright field confocal images (Figure 8). Figure 8 shows a comparison of bright field micrographs, obtained with surface B5 treated with streptavidin (Figure 8a) and surface C once is treated with protein (Figure 8b). As it can be seen, the characteristic red color of the Atto streptavidin chromophore is only observed in the latter, which confirms the protein immobilization on the surface in turn associated with the bioactivation by compound **2**.

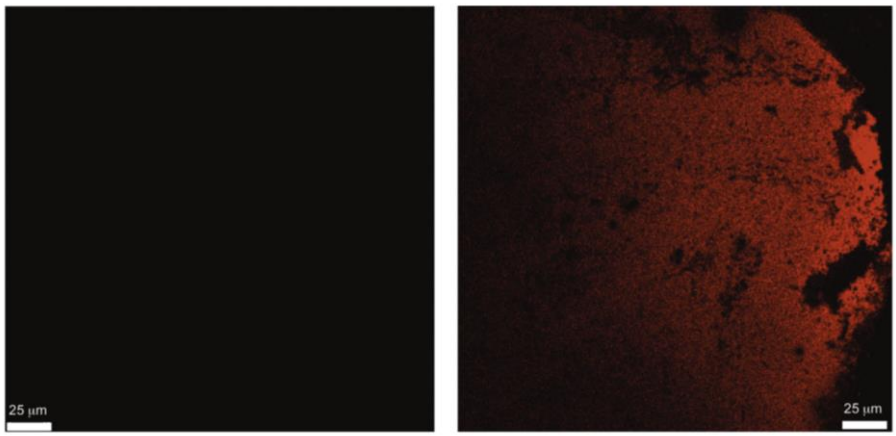

Figure 8. Fluorescent images of modified surfaces incubated with streptavidin. a) Tripod **1** terminated surface B5, without **2** and treated with streptavidin. No protein adhesion was observed. b) Surface C treated with streptavidin, its presence is revealed by the characteristic red spots.

Versatility of modified surfaces offers the possibility of using theophylline derivatives as an alternative to the surface activation, by chemical grafting, to study receptor-ligand interactions without false positives (according to Hunt et al.)[34] and improving biochemical sensor devices for the protein immobilization.[35]

4. Conclusions.

In this work we have presented the covalent bond of a tripod-shaped penta(*p*-phenylene) (**1**) on silicon surface as template for the specific incorporation of proteins. We synthesized azido-functionalized penta(*p*-phenylene) that have been immobilized on alkynyl-terminated Si wafers by CuAAc reaction. Several conditions have been optimized to find the best tripod-modified surface in terms of surface density, aggregation and tripod configuration, which were determined by XPS and AFM analysis. The height of the tripodal structures deposited on the Si wafer was theoretically calculated by using density functional theory. These data confirmed that the height profile extracted from AFM analysis corresponding to the deposited penta(*p*-phenylene) molecules depends on the conformation of azide groups attached on the alkynyl-terminated Si surface. We also used CuAAC reaction to attach a theophylline derivative onto the tripod-modified surfaces. The covalent incorporation of the azido-terminated theophylline **2** was confirmed by fluorescence microscopy and XPS after binding with streptavidin protein. This easy and reproducible methodology offers the possibility for the specific incorporation of proteins in potential application in cell attachment.

5. Acknowledgments.

The authors wish to thank the financial support to the Spanish Ministerio de Economía y Competitividad, Projects CTQ13-48418-P and CTQ16-76311-R, FEDER funds.

6. References.

1 (a) A. J. Pertsin, M. Grunze, H. J. Kreuzer, R. L. C. Wang, The effect of electrostatic fields on an oligo(ethylene glycol) terminated alkanethiol self-assembled monolayer, Phys. Chem. Chem. Phys. 2 (2000) 1729-1733.

(b) J. Frommer, R. Luthi, E. Meyer, D. Anselmetti, M. Dreier, R. Overney, H. J. Guntherodt, M. Fujihira, Adsorption at domain edges, Nature 364 (1993) 198-213.

(c) C. Roberts, C. S. Chen, M. Mrksich, V. Martichonok, D. E. Ingber, G. M. Whitesides, Using mixed self-Assembled monolayers presenting RGD and $(EG)_3OH$ groups to characterize long-term attachment of bovine capillary endothelial cells to surfaces, J. Am. Chem. Soc. 120 (1998) 6548-6555.

(d) G. B. Sigal, C. Bamdad, A. Barberis, J. Strominger, G. M. Whitesides, A self-assembled monolayer for the binding and study of histidine-tagged proteins by surface plasmon resonance, Anal. Chem. 68 (1996) 490-497.

(e) G. P. López, M. W. Albers, S. L. Schreiber, R. Carroll, E. Peralta, G. M. Whitesides, Convenient methods for patterning the adhesion of mammalian cells to surfaces using self-assembled monolayers of alkanethiolates on gold, J. Am. Chem. Soc. 115 (1993) 5877-5878.

(f) M. C. Pirrung, How to make a DNA chip, Angew. Chem., Int. Ed. 41 (2002) 1276-1289.

(g) D. S. Wilson, S. Nock, Recent developments in protein microarray technology, Angew. Chem., Int. Ed. 42 (2003) 494-500.

2 S. W. Schmitt, F. Schechtel, D. Amkreutz, M. Bashouti, S. K. Srivastava, B. Hoffmann, C. Dieker, E. Spiecker, B. Rech, S. H. Christiansen, Nanowire arrays in multicrystalline silicon thin films on glass: a promising material for research and applications in nanotechnology, Nano Lett. 12 (2012) 4050−4054.

3 T. Yokoyama, S. Yokoyama, T. Kamikado, Y. Okuno, S. Mashiko, Selective assembly on a surface of supramolecular aggregates with controlled size and shape, Nature 413 (2001) 619-621.

4 V. Paraschiv, S. Zapotoczny, M. R. Jong de, G. J. Vancso, J. Huskens, D. N. Reinhoudt, Functional group transfer from gold nanoparticles to flat gold surfaces for the creation of molecular anchoring points on surfaces, Adv. Mater. 14 (2002) 722–726.

5 M. E. Drew, A. Chworos, E. Oroudjev, H. Hansma, Y. Yamakoshi, A tripod molecular tip for single molecule ligand−receptor force spectroscopy by AFM, Langmuir 26 (2010) 7117–7125.

6 (a) H. Fabre, D. Mercier, A. Galtayries, D. Portet, N. Delorme, J. F. Bardeau. Appl. Surf. Sci. (2017) http://dx.doi.org/10.1016/j.apsusc.2017.08.138.

(b) N. Ballav, A. Terfort, M. Zharnikov, Fabrication of mixed self-assembled monolayers designed for avidin immobilization by irradiation promoted exchange reaction, Langmuir, 25 (2009) 9189-9196.

(c) A. Dkhissi, A. Esteve, M. Djafari-Rouhani, L. Jeloaica, Understanding the microscopic structure of SAMs/SiO_2 interfaces in the presence of water using first-principles modeling, J. Phys. Chem. C, 112 (2008) 5567-5572.

(d) L. R. Hochberg, M. D. Serruya, G. M. Friehs, J. A. Mukand, M. Saleh, A. H. Caplan, A. Branner, D. Chen, R. D. Penn, J. P. Donoghue, Neuronal ensemble control of prosthetic devices by a human with tetraplegia, Nature, 442 (2006) 164-171.

7 H.-I. Chang, Y. Wang, in Regenerative Medicine and Tissue Engineering-Cells and Biomaterials, Vol. 1, 1st ed. (Ed.: D. Eberli), InTech, Rijeka, Croatia, 2011, pp. 569.

8 J. Thomas, Parsons, A. R. Horwitz, M. A. Schwartz, Cell adhesion: integrating cytoskeletal dynamics and cellular tension, Nat. Rev. Mol. Cell Biol. 11 (2010) 633-644.

9 M. Abedin, N. King, Diverse evolutionary paths to cell adhesion Trends Cell Biol. 20, (2010) 734-742.

10 J. L. Cannons, H. Qi, K. T. Lu, M. Dutta, J. Gomez-Rodriguez, J. Cheng, E. K. Wakeland, R. N. Germain, P. L. Schwartzberg, Optimal germinal center responses require a multistage T cell: B cell adhesion process involving integrins, SLAM-associated protein, and CD84, Immunity 32 (2010) 253-265 .

11 J. A. Callow, M. E. Callow, Trends in the development of environmentally friendly fouling-resistant marine coatings, Nat. Commun. 2 (2011) 1-10.

12 (a) G. Lovat, D. Forrer, M. Abadia, M. Dominguez, M. Casarin, C. Rogero, A. Vittadini, L. Floreano, Hydrogen capture by porphyrins at the TiO_2(110) surface, Phys. Chem. Chem. Phys. 17 (2015) 30119-30124.

(b) J. S. Lindney, S. Prathapan, T. E. Johnson, R. W. Wagner, Porphyrin building blocks for modular construction of bioorganic model systems, Tetrahedron 50 (1994) 8941-8968.

13 (a) S. Ulrich, U. Jung, U.; T. Strunskus, C. Schütt, A. Bloedorn, S. Lemke, E. Ludwig, L. Kipp, F. Faupel, O. Magnussen, R Herges, X-ray spectroscopy characterization of azobenzene-functionalized triazatriangulenium adlayers on Au(111) surfaces, Phys. Chem. Chem. Phys. 17 (2015) 17053-17062.

(b) B. Baisch, D. Raffa, U. Jung, O. M. Magnussen, C. Nicolas, J. Lacour, J. Kubitschke, R. Herges, Mounting freestanding molecular functions onto surfaces: the platform approach, J. Am. Chem. Soc. 131 (2009) 442-443.

14 V. Percec, E. Aqad, M. Peterca, J. G. Rudick, L. Lemon, J. C. Ronda, B. B. De, P. A. Heiney, E. W. Meijer, Steric communication of chiral information observed in dendronized polyacetylenes J. Am. Chem. Soc. 128 (2006) 16365-16372.

15 (a) D. Jishkariani, Y. Wu, D. Wang, Y. Liu, A. Blaaderen, C. B. Murray, Preparation and self-assembly of dendronized Janus Fe_3O_4-Pt and Fe_3O_4-Au heterodimers, ACS Nano 11 (2017) 7958-7966.

(b) N. G. García-Peña, A. Caminade, A. Ouali, R. Redon, C. Turrin, Solventless synthesis of Ru(0) composites stabilized with polyphosphorhydrazone (PPH) dendrons and their use in catalysis, RSC Adv. 6 (2016) 64557-64567.

16 (a) X. Deng, A. Mayeux, C. Cai, An efficient convergent synthesis of novel anisotropic

adsorbates based on nanometer-sized and tripod-shaped oligophenylenes end-capped with triallylsilyl groups, J. Org. Chem. 67 (2002) 5279-5283.

(b) J. Hierrezuelo, E. Guillén, J. M. López-Romero, R. Rico, M.R. López-Ramírez, J. C. Otero, C. Cai, Synthesis and structural analysis of substituted tripod-Shaped tri- and tetra(p-phenylene)s, Eur. J. Org. Chem. 29 (2010) 5672-5680.

(c) J. Hierrezuelo, R. Rico, M. Valpuesta, A. Díaz, J. M. López-Romero, M. Rutkis, J. Kreigberga, V. Kampars, M. Algarra, Synthesis of azobenzene substituted tripod-Shaped bi(*p*-phenylene)s. Adsorption on gold and CdS quantum-dots surfaces, Tetrahedron 69 (2013) 3465-3474.

17 (a) C. Lee, Y. Zhang, A. Romayanantakit, E. Galoppini, Modular synthesis of ruthenium tripodal system with variable anchoring groups positions for semiconductor sensitization, Tetrahedron 66 (2010) 3897-3903.

(b) Y. X. Yao, J. M. Tour, Facile convergent route to molecular caltrops, J. Org. Chem. 64 (1999) 1968-1970.

(c) Y. Shirai, J. M. Guerrero, T. Sasaki, T. He, H. Ding, G. Vives, B. C. Yu, L. Cheng, A. K. Flatt, P. G. Taylor, Y. Gao, J. M. Tour, Fullerene/thiol-terminated molecules, J. Org. Chem. 74 (2009) 7885-7900.

18 H. C. Kolb, M. Finn, K. B. Sharpless, Click chemistry: diverse chemical function from a few good reactions, Angew. Chem. Int. Ed. 40 (2001) 2004-2021.

19 (a) R. D. Rohde, H. D, Agnew, W.-S. Yeo, R. C. Bailey, J. R. Heath, A non-oxidative approach toward chemically and electrochemically functionalizing Si(111), J. Am. Chem. Soc. 128 (2006) 9518-9525.

(b) S. Ciampi, G. Le Saux, J. B. Harper, J. J. Gooding, Optimization of click chemistry of ferrocene derivatives on acetylene-functionalized silicon(100) surfaces, Electroanalysis 20 (2008) 1513-1519.

(c) G. Quin, C. Santos, W. Zhang, Y. Lin, A. Kumar, U. J. Erasquin, K. Liu, P. Muradov, B. Wells Trautner, C. Cai. Biofunctionalization on alkylated silicon substrate surfaces via "click" chemistry, J. Am. Chem. Soc. 132 (2010) 16432-16441.

(d) P. Michaels, M. T. Alam, S. Ciampi, W. Rouesnel, S. G. Parker, M. H. Choudhury, J. J. Gooding, A robust DNA interface on a silicon electrode, Chem. Commun. 50 (2014) 7878-7880.

20 M. Sánchez-Molina, J.M. López-Romero, J. Hierrezuelo-León, M. Martín-Rufián, A. Díaz, M. Valpuesta, R. Contreras-Cáceres, Synthesis and Covalent Grafting of Tripod-Shaped Oligo(*p*-phenylene)s End-Capped with Azide Groups, Asian J. Org. Chem. 5 (2016) 550-559.

21 R. Langer, R. D. A. Tirrell, Designing materials for biology and medicine, Nature 428 (2004) 487-492.

22 A. Hartl, E. Schmich, J. A. Garrido, J. Hernando, S. C. R. Catharino, S. Walter, P. Feulner, A. Kromka, D. Steinmuller, M. Stutzmann, Protein-modified nanocrystalline diamond thin films for biosensor applications, Nat. Mater 3 (2004) 736-742.

23 D. G. Castner, B. D. Ratner, Biomedical surface science: foundations to frontiers, Surf. Sci. 500 (2002) 28-60.

24 J. Hierrezuelo, V. Romero, J. Benavente, R. Rico, J.M. López-Romero, Membrane surface functionalization *via* theophylline derivative coating and streptavidin immobilization, Colloids and Surfaces B: Biointerfaces 113 (2014) 176-181.

25 R. Suau, R. Rico, F. Nájera, F. J. O. López, J. M. López-Romero, M. Moreno-Mañas, A. Roglans, The palladium(0) Suzuki cross-coupling reaction as the key step in the synthesis of aporphinoids, Tetrahedron 60 (2004) 5725-5735.

26 Y. Li, J. Wang, C. Cai, Rapid grafting of azido-labeled oligo(ethylene glycol)s onto an alkynyl-terminated monolayer on nonoxidized silicon via microwave-assisted "click" reaction, Langmuir 27 (2011) 2437-2445.

27 C. M. Yam, C. Cai, Thin films derived from giant, tripod-shaped oligophenylenes end-capped with triallylsilyl groups on hydrogen-terminated Si(111) surfaces, Colloid Interface Sci. 301 (2006) 441-445.

28 A. Lucena-Serrano, C. Lucena-Serrano, R. Contreras-Cáceres, A. Díaz, M. Valpuesta, C. Cai, J. M. López-Romero, Silicon surface biofunctionalization with dopaminergic tetrahydroisoquinoline derivatives, Appl. Surf. Sci. 360 (2016) 419-428.

29 S. Nafisi, F. Manouchehri, H.-A. Tajmir-Riahi, M. J. Varavipour, Structural features of DNA interaction with caffeine and theophylline, J. Mol. Struct. 875 (2008) 392-399.

30 M. Legraverend, D. S. Grierson, The purines: Potent and versatile small molecule inhibitors and modulators of key biological targets, Bioorg. Med. Chem. 14 (2006) 3987-4006.

31 J. A. Ribeiro, A. M. Sebastião, A. Mendonça, Adenosine receptors in the nervous system: pathophysiological implications, Prog. Neurobiol. 68 (2003) 377-392.

32 J. Hierrezuelo, J. M. López-Romero, R. Rico, J. Brea, M. I. Loza, C. Cai, M. Algarra, Synthesis of theophylline derivatives and study of their activity as antagonists at adenosine receptors, Bioorg. Med. Chem. 18 (2010) 2081-2088.

33 M. I. Vázquez, V. Romero, J. Benavente, R. Romero, J. Hierrezuelo, J. M. López-Romero, R. Contreras-Cáceres, Characterization and stability of a bioactivated alumina nanomembrane for application in flow devices, Microporous Mesoporous Mater. 226 (2016) 88-93.

34 J. L. Dahmen, Y. Yang, C. M. Greenlief, G. Stacey, H. K. Hunt, Interfacing Whispering Gallery Mode Optical Microresonator Biosensors with the Plant Defense Elicitor Chitin, Colloids Surf. B 122 (2014) 241-249.

35 G. Vitola, R. Mazzei, E. Fontananova, L. Giorno, PVDF membrane biofunctionalization by chemical grafting, J. Membr. Sci. 476 (2015) 483-489.